MPC with Sliding Mode Control for the Energy Management System of Microgrids ⋆

Gian Paolo Incremona * **Michele Cucuzzella** ** **Lalo Magni** *
Antonella Ferrara **

* *Dipartimento di Ingegneria Civile e Architettura, University of Pavia, 27100 Italy (e-mail: gp.incremona@gmail.com, lalo.magni@unipv.it).*
** *Dipartimento di Ingegneria Industriale e dell'Informazione, University of Pavia, 27100 (e-mail: michele.cucuzzella@gmail.com, antonella.ferrara@unipv.it)*

Abstract: This paper presents the design of a high level Model Predictive Control (MPC) for efficient management and consumption of energy resources in microgrids locally controlled via Sliding Mode Control (SMC). The proposed MPC relies on a new model of the so-called Energy Management System (EMS), which takes into account the involved powers as new inputs. In the paper, the microgrid includes a Distributed Generation unit (DGu), based on a renewable energy source, and two Energy Storage units (ESus), working both in grid-connected and islanded operation mode and controlled by SMC. The MPC module generates the references of power for the energy storage systems, taking into account input and state constraints. The proposed approach is theoretically analyzed and the asymptotical stability of the controlled systems is proved. Simulation assessment confirms the efficacy of the proposal.

Keywords: Predictive control, sliding mode control, uncertain dynamic systems, electric power systems.

1. INTRODUCTION

In the last decades, the main trends in power systems focus on the development of a resilient and smart architecture for the energy generation and distribution. In this context, the terms "microgrid" and "smart grid" represent the main keywords of a new paradigm in which energy technologies and optimization methods for power systems play a particularly relevant role [Amin and Wollenberg, 2005].

A microgrid is a set of multiple mutual connected distributed generation units (DGus), which are usually close to the energy consumers [Lasseter, 2002]. Since there is need to monitor and control the geographically dispersed DGus in a efficient and reliable way, a kind of supervisor, called Energy Management System (EMS), is normally utilized. It consists of computer tools and utilities to monitor, control and guarantee the security and the reliability of the overall grid [Palma-Behnke et al., 2013; Tan et al., 2013; Rahimi-Eichi et al., 2013]. It can also include applications to provide adaptive demand forecasting. In this paper, we focus on the control function of the EMS, specifically addressing the problem of the correct generation of the reference signals for the Energy Storage units (ESus) usually present in microgrids.

In the literature, several control strategies have been proposed to optimize the microgrid performance, in both grid-connected operation mode (GCOM) and islanded operation mode (IOM), as discussed for instance in [Bouzid et al., 2015] and in the references therein.

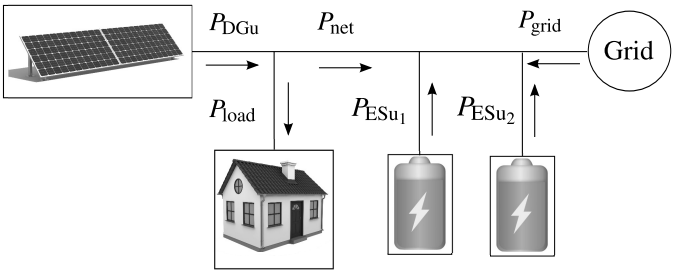

Fig. 1. Power flows in the considered microgrid.

One of the main challenges that the design of microgrid controllers has to face is the presence of modelling uncertainties and external disturbances, for instance due to the use of voltage-source-converters (VSCs) as interface media between the DGus and the main grid. This is why the adoption of robust control methodologies is advisable in field implementations. Sliding Mode Control (SMC) represents a valid robust control solution able to reject a class of uncertainties frequently encountered in real word systems [Utkin, 1992]. This methodology was already applied with satisfactory results in case of power systems control, as illustrated in [Cucuzzella et al., 2015a,b,c, 2016, 2017; Trip et al., 2017; Incremona et al., 2016].

In reality, apart from the basic control requirements, microgrids often requires to satisfy some input and state constraints so that the use of optimal control techniques results in being the more effective way to solve the associated control problem. Model Predictive Control (MPC) [Rawlings and Mayne, 2009; Mayne, 2014] is widely used to search for an optimal control solution, while fulfilling the constraints on the basis of a suitable predictor of the plant behavior. For this reason it can be regarded as

⋆ This is the final version of the accepted paper submitted for inclusion in the Proceedings of the International Federation of Automatic Control (IFAC) World Congress, Toulouse, France, July, 2017.

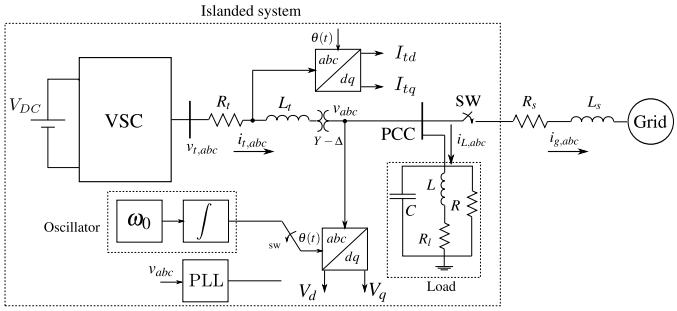

Fig. 2. Single-line diagram of a generic DGu or ESu.

an eligible approach even in case of microgrids. Note that the combined use of MPC and SMC was already investigated in [Incremona et al., 2017a,b].

In this paper, we propose a different control architecture having a supervisory control structure still based on the joint use of MPC and SMC. The proposed scheme is tailored for a microgrid including a DGu with a renewable energy source and two Energy Storage units (ESus), as schematically shown in Figure 1, but the concept could be easily extended to more complex microgrids.

In our proposal, the low level controller implements a second-order sliding mode control strategy, belonging to the class of Suboptimal algorithms (SSOSM) [Bartolini et al., 1998]. It is valid for both the GCOM and the IOM. This low level controller is used to track the power references generated by an high level MPC component. The latter has to take into account the limits on the State of Charge (SoC) of the ESus, as well as the net power exchanged among the elements of the power network. Note that, the MPC element is based on a new model of the considered EMS, which, differently from other proposals in the literature (see for instance [Palma-Behnke et al., 2013] and the references therein), regards the ESus powers as new inputs, instead of dealing only with their variations.

In the paper we prove that the system controlled via the proposed control strategy is asymptotically stable. Simulation results referred to a realistic scenario are provided to confirm the effectiveness of the proposed hierarchical MPC/SMC scheme.

The present paper is organized as follows. In Section 2 some preliminary issues on the considered microgrid and EMS model are discussed and the problem is formulated. In Section 3 the proposed low level SSOSM controller and the high level MPC module are presented. They are theoretically analyzed in Section 4. A realistic simulation case study is presented in Section 5, while some conclusions are gathered in Section 6.

2. PROBLEM FORMULATION

Figure 1 represents the considered microgrid with all its elements, while Figure 2 schematically illustrates the considered DGus or ESus. For a detailed description of the considered variables, the value of which are reported in Table 1, the readers can refer to [Cucuzzella et al., 2015a]. Note that, in the following, both the model in GCOM and the model in IOM will be considered. In GCOM, the Point of Common Coupling (PCC) voltage amplitude and frequency are fixed by the main grid and the system works in stiff synchronization with the grid by using the so-called phase-locked-loop (PLL) device. In IOM, the circuit breaker (named SW in Figure 2) is open. Because

Table 1. Electrical parameters of the DGu/ESu

Quantity	Value	Description
$V_{\rm DC}$	1000 V	DC voltage source
$f_{\rm c}$	10 kHz	PWM carrier frequency
R_t	40 mΩ	VSC filter resistance
L_t	10 mH	VSC filter inductance
R_s	0.1 Ω	Grid resistance
f_0	60 Hz	Nominal grid frequency
$V_{\rm n}$	120 V	Nominal grid phase-voltage (RMS)

of the power mismatch between the DGu or ESus and the load, the PCC voltage and frequency could deviate from the nominal values. Therefore, in IOM, one of the ESu serves as master unit and it provides a suitable current to the shared three-phase parallel resistive-inductive-capacitive (*RLC*) load, in order to keep the voltage of the microgrid equal to the nominal value. Note that, in this paper, we assume that the master ESu has an appropriate capacity to supply the microgrid load in IOM.

2.1 Model in GCOM

Making reference to the stationary *abc*-frame, the dynamics equations of the energy units in GCOM are the following

$$\begin{cases} i_{t,abc} = \frac{1}{R} v_{abc} + i_{L,abc} + C\frac{dv_{abc}}{dt} + i_{g,abc} \\ v_{t,abc} = L_t \frac{di_{t,abc}}{dt} + R_t i_{t,abc} + v_{abc} \\ v_{abc} = L\frac{di_{L,abc}}{dt} + R_l i_{L,abc} = L_s \frac{di_{g,abc}}{dt} + R_s i_{g,abc} + v_{g,abc} \end{cases} \tag{1}$$

where $i_{t,abc}$, v_{abc}, $i_{L,abc}$, $i_{g,abc}$, $v_{t,abc}$ and $v_{g,abc}$ are 3×1 vectors, containing the corresponding quantities of each phase. In particular, these represent the currents delivered by the energy unit, the load voltages, the currents fed into the load inductance (L), the currents exchanged with the main grid, the VSC output voltages and the grid voltages, respectively.

Each three-phase variable of (1) can be converted into the synchronous rotating dq-frame by applying the Clarke's and Park's transformations. Then, the so-called state-space representation of (1) results in being

$$\begin{cases} \dot{x}_1(t) = -\frac{1}{RC}x_1(t) + \omega x_2(t) + \frac{1}{C}x_3(t) - \frac{1}{C}x_5(t) - \frac{1}{C}x_7(t) \\ \dot{x}_2(t) = -\omega x_1(t) - \frac{1}{RC}x_2(t) + \frac{1}{C}x_4(t) - \frac{1}{C}x_6(t) - \frac{1}{C}x_8(t) \\ \dot{x}_3(t) = -\frac{1}{L_t}x_1(t) - \frac{R_t}{L_t}x_3(t) + \omega x_4(t) + \frac{1}{L_t}u_1(t) \\ \dot{x}_4(t) = -\frac{1}{L_t}x_2(t) - \omega x_3(t) - \frac{R_t}{L_t}x_4(t) + \frac{1}{L_t}u_2(t) \\ \dot{x}_5(t) = \frac{1}{L}x_1(t) - \frac{R_l}{L}x_5(t) + \omega x_6(t) \\ \dot{x}_6(t) = \frac{1}{L}x_2(t) - \omega x_5(t) - \frac{R_l}{L}x_6(t) \\ \dot{x}_7(t) = \frac{1}{L_s}x_1(t) - \frac{R_s}{L_s}x_7(t) + \omega x_8(t) - \frac{1}{L_s}u_3(t) \\ \dot{x}_8(t) = \frac{1}{L_s}x_2(t) - \omega x_7(t) - \frac{R_s}{L_s}x_8(t) - \frac{1}{L_s}u_4(t) \\ y_{d\,\rm GCOM}(t) = x_3(t) \\ y_{q\,\rm GCOM}(t) = x_4(t) \end{cases} \tag{2}$$

where $x = [V_d\ V_q\ I_{td}\ I_{tq}\ I_{Ld}\ I_{Lq}\ I_{gd}\ I_{gq}]^T \in \mathcal{X} \subset \mathbb{R}^8$ is the state variables vector, $u = [V_{td}\ V_{tq}\ V_{gd}\ V_{gq}]^T \in \mathcal{U} \subset \mathbb{R}^4$ is the input vector and $y_{\rm GCOM} = [I_{td}\ I_{tq}]^T \in \mathbb{R}^2$ is the output vector. The inputs $u_3 = V_{gd}$ and $u_4 = V_{gq}$ are the components of the control vector due to the presence of the main grid in the model.

Assume now that the overall load is predominantly resistive, as it often happens in real distribution power systems. Then, the equations of the EMS in GCOM can be written from the balance of the involved active powers as schematized in Figure 1, i.e.,

$$P_{\rm net} + P_{\rm ESu_1} + P_{\rm ESu_2} + P_{\rm grid} = 0 \tag{3}$$

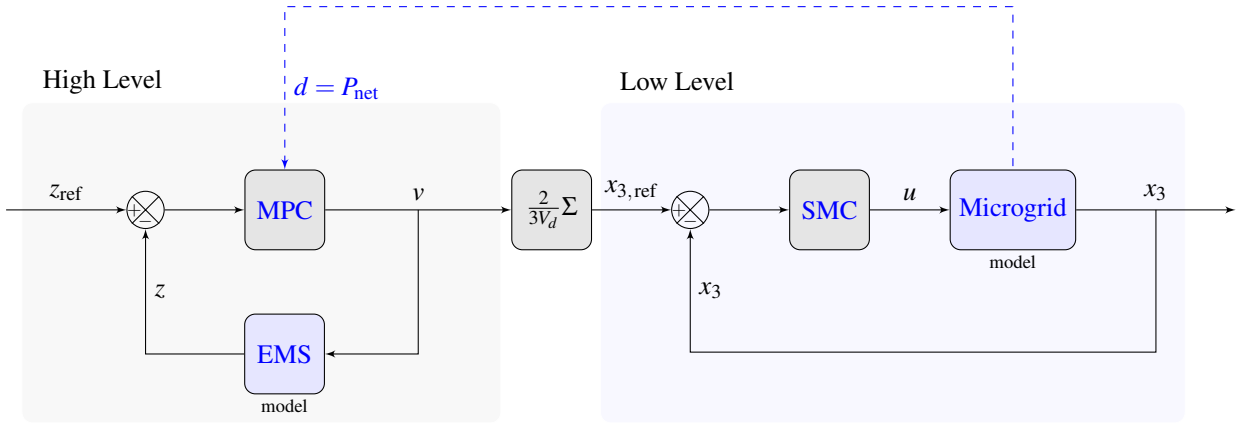

Fig. 3. Hierarchical MPC/SMC control scheme.

where $P_{\text{net}} = P_{\text{DGu}} - P_{\text{load}}$ is the net power given by the difference between the power generated by the DGu and that required by the load, P_{ESu_i}, $i = 1,2$, are the powers delivered by the ESus, while P_{grid} is the power absorbed from the grid. The corresponding discrete-time linear EMS model can be expressed as follows

$$\begin{cases} SoC_1(k+1) = SoC_1(k) - \alpha_1 P_{\text{ESu}_1}(k) \\ SoC_2(k+1) = SoC_2(k) - \alpha_2 P_{\text{ESu}_2}(k) \\ P_{\text{grid}}(k+1) = P_{\text{grid}}(k) + \Delta P_{\text{grid}}(k) \end{cases} \tag{4}$$

such that

$$P_{\text{grid}}(k) = -P_{\text{net}}(k) - P_{\text{ESu}_1}(k) - P_{\text{ESu}_2}(k) \tag{5}$$

where $k \in \mathbb{N}_0$ is the discrete time instant, while α_i is a coefficient that expresses the relationship between the power and the SoC of the ESus. Specifically, given the sampling time T, α_i can be expressed as $\alpha_i = \eta_{\text{ESu}_i} T / C_{\text{ESu}_i}$, with η_{ESu_i} and C_{ESu_i} being the efficiency and the energy capacity of the i-th ESu, respectively. The state-space representation is instead the following

$$\begin{cases} z_1(k+1) = z_1(k) - \alpha_1 v_1(k) \\ z_2(k+1) = z_2(k) - \alpha_2 v_2(k) \\ z_3(k+1) = z_3(k) + v_3(k) \\ y_{\text{EMS},1}(k) = z_1(k) \\ y_{\text{EMS},2}(k) = z_2(k) \\ y_{\text{EMS},3}(k) = z_3(k) \end{cases} \tag{6}$$

such that it holds $z_3 = -d - v_1 - v_2$, where the state vector is $z = [SoC_1\ SoC_2\ P_{\text{grid}}]^T \in \mathcal{Z} \subset \mathbb{R}^3$. Then, $v = [P_{\text{ESu}_1}\ P_{\text{ESu}_2}\ \Delta P_{\text{grid}}]^T \in \mathcal{V} \subset \mathbb{R}^3$ is the input vector, $y_{\text{EMS}} = z \in \mathbb{R}^3$ is the output, while $d = P_{\text{net}}$ is considered as a measurable disturbance term.

2.2 Model in IOM

Analogously to the GCOM case, in IOM, referring to the stationary *abc*-frame, the master DGu (or ESu) dynamics equations are

$$\begin{cases} i_{t,abc} = \frac{1}{R} v_{abc} + i_{L,abc} + C \frac{dv_{abc}}{dt} \\ v_{t,abc} = L_t \frac{di_{t,abc}}{dt} + R_t i_{t,abc} + v_{abc} \\ v_{abc} = L \frac{di_{L,abc}}{dt} + R_l i_{L,abc} \end{cases} \tag{7}$$

while, according to the synchronous rotating dq-frame (with θ provided by the internal oscillator set to ω_0), the state-space representation of (7) is

$$\begin{cases} \dot{x}_1(t) = -\frac{1}{RC} x_1(t) + \omega_0 x_2(t) + \frac{1}{C} x_3(t) - \frac{1}{C} x_5(t) \\ \dot{x}_2(t) = -\omega_0 x_1(t) - \frac{1}{RC} x_2(t) + \frac{1}{C} x_4(t) - \frac{1}{C} x_6(t) \\ \dot{x}_3(t) = -\frac{1}{L_t} x_1(t) - \frac{R_t}{L_t} x_3(t) + \omega_0 x_4(t) + \frac{1}{L_t} u_1(t) \\ \dot{x}_4(t) = -\frac{1}{L_t} x_2(t) - \omega_0 x_3(t) - \frac{R_t}{L_t} x_4(t) + \frac{1}{L_t} u_2(t) \\ \dot{x}_5(t) = \frac{1}{L} x_1(t) - \frac{R_l}{L} x_5(t) + \omega_0 x_6(t) \\ \dot{x}_6(t) = \frac{1}{L} x_2(t) - \omega_0 x_5(t) - \frac{R_l}{L} x_6(t) \\ y_{d\,\text{IOM}}(t) = x_1(t) \\ y_{q\,\text{IOM}}(t) = x_2(t) \end{cases} \tag{8}$$

where $x = [V_d\ V_q\ I_{td}\ I_{tq}\ I_{Ld}\ I_{Lq}]^T \in \mathcal{X} \subset \mathbb{R}^6$ is the state vector, $u = [V_{td}\ V_{tq}]^T \in \mathcal{U} \subset \mathbb{R}^2$ is the input vector and $y_{\text{IOM}} = [V_d\ V_q]^T \in \mathbb{R}^2$ is the output vector.

The corresponding equations of the EMS in IOM are instead the following

$$\begin{cases} SoC_1(k+1) = SoC_1(k) - \alpha_1 P_{\text{ESu}_1}(k) \\ SoC_2(k+1) = SoC_2(k) - \alpha_2 P_{\text{ESu}_2}(k) \end{cases} \tag{9}$$

with

$$P_{\text{ESu}_1}(k) = -P_{\text{net}}(k) - P_{\text{ESu}_2}(k) \tag{10}$$

The corresponding state-space representation is

$$\begin{cases} z_1(k+1) = z_1(k) - \alpha_1 v_1(k) \\ z_2(k+1) = z_2(k) - \alpha_2 v_2(k) \\ y_{\text{EMS},1}(k) = z_1(k) \\ y_{\text{EMS},2}(k) = z_2(k) \end{cases} \tag{11}$$

such that $v_1 = -d - v_2$, where $z = [SoC_1\ SoC_2]^T \in \mathcal{Z} \subset \mathbb{R}^2$ is the state vector, $v = [P_{\text{ESu}_1}\ P_{\text{ESu}_2}]^T \in \mathcal{V} \subset \mathbb{R}^2$ is the input vector, while $y_{\text{EMS}} = z$ is the output. Note that, we can assume, for instance, that the ESu_1 has the role of master unit.

2.3 Problem Statement

The control problem to solve can be now formulated: *i) in GCOM, design a control scheme able to generate the optimal power references for the ESus of the microgrid, in order to minimize the power exchanged with the main grid; ii) in IOM, the control scheme has to be able to minimize the power delivered by the ESu that assumes the role of master unit.*

3. THE PROPOSED CONTROL SCHEME

In this section, the hierarchical MPC/SMC scheme illustrated in Figure 3 is discussed.

3.1 The Sliding Mode Control Component

The considered SSOSM control strategy is of the same form discussed in [Cucuzzella et al., 2015a]. For the sake of brevity, due to space limitations, the SSOSM control laws in GCOM and IOM will be briefly recalled.

In GCOM, the so-called sliding variables are set as the error of I_{td} and I_{tq} with respect to their references, i.e.,

$$\sigma_{d_{\text{GCOM}}}(t) = y_{d_{\text{GCOM}},\text{ref}} - y_{d_{\text{GCOM}}}(t) \tag{12}$$

$$\sigma_{q_{\text{GCOM}}}(t) = y_{q_{\text{GCOM}},\text{ref}} - y_{q_{\text{GCOM}}}(t) \tag{13}$$

Since the relative degree r of the system is equal to 1, in order to alleviate the so-called chattering phenomenon, a SSOSM can be applied, following the design procedure presented in [Cucuzzella et al., 2015a]. The control laws, to steer $\sigma_{i,1_{\text{GCOM}}}$, $i = d,q$, and its first time derivative to zero in a finite time in spite of the uncertainties, is the following

$$w_{i_{\text{GCOM}}} = -\alpha_{i_{\text{GCOM}}} U_{i_{\text{GCOM,max}}} \operatorname{sgn}\left(\sigma_{i,1_{\text{GCOM}}} - \tfrac{1}{2}\sigma_{i,1_{\text{GCOM,max}}}\right) \tag{14}$$

where $w_{i_{\text{GCOM}}} = \dot{u}_{i_{\text{GCOM}}}$ is the auxiliary control variable such that $u_{i_{\text{GCOM}}}$, $i = d,q$, are continuous, while $\alpha_{i_{\text{GCOM}}} > 0$, and $U_{i_{\text{GCOM,max}}} > 0$ are suitably chosen in order to enforce a sliding mode.

Analogously, in IOM, the sliding variables associated to the master ESu are chosen as

$$\sigma_{d_{\text{IOM}}}(t) = y_{d_{\text{IOM}},\text{ref}} - y_{d_{\text{IOM}}}(t) \tag{15}$$

$$\sigma_{q_{\text{IOM}}}(t) = y_{q_{\text{IOM}},\text{ref}} - y_{q_{\text{IOM}}}(t) \tag{16}$$

With reference to (15)-(16), the relative degree r is equal to 2 so that a SSOSM naturally applies. In this case, the control law is

$$u_{i_{\text{IOM}}} = -\alpha_{i_{\text{IOM}}} U_{i_{\text{IOM,max}}} \operatorname{sgn}\left(\sigma_{i,1_{\text{IOM}}} - \tfrac{1}{2}\sigma_{i,1_{\text{IOM,max}}}\right) \tag{17}$$

with $\alpha_{i_{\text{IOM}}} > 0$ and $U_{i_{\text{IOM,max}}} > 0$ being suitably chosen so as to enforce a sliding mode. Note that, in order to obtain chattering alleviation, one can refer to third order sliding mode control algorithm presented in [Cucuzzella et al., 2015a].

3.2 The Model Predictive Control Component

The MPC component has the role to generate the power references for the SSOSM low level controllers in Figure 3, while respecting some constraints in terms of powers and SoC. More precisely, in order to generate the references of the current (d-component) for both ESus, we assume that $x_{3,\text{ref}} = 2/(3V_d)\Sigma v \in \mathbb{R}^2$, $\Sigma \in \mathbb{R}^{2\times 3}$ being a selection matrix having only the two elements $\Sigma_{11} = \Sigma_{22} = 1$ and all the other elements null. The SSOSM controllers have the aim of tracking $x_{3,\text{ref}}$ and rejecting the matched uncertainties, while guaranteeing the stability of the overall system. Note that, in IOM the voltage control (15)-(17) is applied to the master ESu_1.

The MPC controller is designed for system (6) in GCOM or system (11) in IOM. The application of a MPC controller implies to solve the so-called Finite-Horizon Optimal Control Problem (FHOCP) that consists in minimizing, at any sampling time k, with respect to the control sequence $\mathbf{v}_{[k,k+N-1|k]} := [v_0(k),\, v_1(k),\ldots,v_{N-1}(k)]$, $N \geq 1$ being the prediction horizon, a suitably defined cost function, i.e.,

$$\begin{aligned} &J(z(k),\mathbf{v}_{[k,k+N-1|k]},N) = \\ &= \sum_{j=0}^{N-1} \|z(k+j) - z_{\text{ref}}(k+j)\|_Q^2 + \|v(k+j)\|_R^2 \\ &+ \|v_1(k+j) + v_2(k+j) + d(k+j)\|_r^2 \\ &+ \|z(k+N) - z_{\text{ref}}(k+N)\|_\Pi^2 \end{aligned} \tag{18}$$

$z_{\text{ref}} \in \mathcal{Z}_{\text{ref}} \subset \mathcal{Z}$ being the reference values, while the notation $\|\cdot\|_W^2$ stands for the square norm of a vector weighted by a matrix W. The cost function (18) is also subject to the dynamics of system (6) in GCOM or system (11) in IOM, and constraints on states and input variables, i.e.,

$$z(k+i) \in \mathcal{Z} \tag{19}$$

$$v(k+i) \in \mathcal{V} \tag{20}$$

$$z(k+N) \in \mathcal{Z}_{\text{f}} \tag{21}$$

with $i = 1,\ldots,N-1$, and $\mathcal{V}$ being a compact set containing the origin. Moreover, $\mathcal{Z}_{\text{f}}$ is the so-called terminal set such that $z(k+N) \in \mathcal{Z}_{\text{f}}$, with

$$\mathcal{Z}_{\text{f}} := \{z \,|\, \|z - \bar{z}_{\text{ref}}\|_\Pi^2 \leq \rho\}, \quad \mathcal{Z}_{\text{f}} \subseteq \mathcal{Z} \tag{22}$$

for any constant $\bar{z}_{\text{ref}} \in \mathcal{Z}_{\text{ref}}$ such that $(\bar{z}_{\text{ref}}, 0)$ is an equilibrium point for systems (6) in GCOM and (11) in IOM, and with $\mathcal{Z}_{\text{f}}$ containing the origin as an interior point. Note that, the value ρ is a positive real number such that $\forall z(\bar{k}) \in \mathcal{Z}_{\text{f}}$, $\forall k > \bar{k}$ it yields,

$$z(k) \in \mathcal{Z}_{\text{f}} \tag{23}$$

$$\kappa_{\text{f}}(e(k)) \in \mathcal{V} \tag{24}$$

with $e(k) = z(k) - \bar{z}_{\text{ref}}(k)$, and $\kappa_{\text{f}}(e)$ being an auxiliary control law that can be

$$\kappa_{\text{f}}(e(k)) = K_{\text{LQ}} e(k) \tag{25}$$

where K_{LQ} is the control gain of the auxiliary control law, that is a Linear-Quadratic (LQ) controller in our case. In (18), Q and R are positive definite matrices, r is a scalar weight, and Π is the positive definite terminal weight associated with the terminal penalty, that is $V_{\text{f}} = \|e(k+N)\|_\Pi^2$ which is assumed such that

$$\begin{aligned} &V_{\text{f}}(e(k+1)) - V_{\text{f}}(e(k)) + \\ &+ \|e(k)\|_Q^2 + \|\kappa_{\text{f}}(e(k))\|_R^2 + \|v_1(k) + v_2(k) + d(k)\|_r^2 \leq 0 \end{aligned} \tag{26}$$

so as to ensure the stability of the controlled system.

Then, according to the Receding Horizon strategy, the applied control law is the following

$$v(k) = \kappa_{\text{MPC}}(e(k)) \tag{27}$$

where

$$\kappa_{\text{MPC}}(e(k)) := v_0^{\text{o}}(k) \tag{28}$$

with $v_0^{\text{o}}(k)$ the first value at k of the generated optimal control sequence.

4. STABILITY ANALYSIS

With reference to the previously discussed control scheme, we refer to [Cucuzzella et al., 2015a] for the stability proofs of the local SSOSM controllers, while the stability of the EMS controlled via the MPC component is hereafter discussed.

Theorem 1. Given the EMS (6) in GCOM and (11) in IOM, by applying the MPC law (27), obtained solving the FHOCP with cost function (18) subject to the system dynamics and input and state constraints (19)-(21), then, $z = \bar{z}_{\text{ref}}$ results in being an asymptotically stable equilibrium point of the controlled system. □

Proof 1. According to the MPC control theory [Rawlings and Mayne, 2009], the proof is distinguished into two steps: i) the proof of the recursive feasibility, i.e., given an optimal solution at time k, it is always possible to find a solution at time $k+1$ such that all the constraints are satisfied; ii) the proof of the stability.

Step 1 (Feasibility) Given the optimal solution at k, that is $\mathbf{v}^{\mathrm{o}}_{[k,k+N-1|k]} := [v^{\mathrm{o}}_0(k), v^{\mathrm{o}}_1(k), \ldots, v^{\mathrm{o}}_{N-1}(k)]$, applying the Receding Horizon principle, only the first element of the optimal sequence is applied. Then, at the time instant $k+1$ the control sequence

$$\widetilde{\mathbf{v}}_{[k+1,k+N|k+1]} = \begin{cases} \mathbf{v}^{\mathrm{o}}_{[k+1,k+N-1|k]} \\ \kappa_{\mathrm{f}}(e(k+N)) \end{cases} \tag{29}$$

fulfills the constraints (19), (20) and (21). In fact, since $\widetilde{\mathbf{v}}_{[k+1,k+N-1|k+1]} = \mathbf{v}^{\mathrm{o}}_{[k+1,k+N-1|k]}$, constraints (19) and (20) are fulfilled. Moreover, from (21), it holds that $z(k+N) \in \mathcal{Z}_{\mathrm{f}}$. Hence, from (23) and (24), it also holds that $\kappa_{\mathrm{f}}(e(k+N)) \in \mathcal{V}$ and $z(k+N) \in \mathcal{Z}$, so that (19) and (20) are satisfied also when $i = N$. Finally, from (23), it follows that $z(k+N+1) \in \mathcal{Z}_{\mathrm{f}}$, which proves the feasibility.

Step 2 (Stability) In order to prove the asymptotical stability of the controlled system, a Lyapunov function candidate has to be chosen. The function $J^{\mathrm{o}}(e(k),k) > 0, \forall\, e \neq 0$, and $J^{\mathrm{o}}(0,k) = 0$, associated with the cost function (18) is a good candidate. Consider the cost function $\widetilde{J}(e(k+1),k+1)$ associated with the feasible control sequence (29). Note that, this function is not a priori the optimal one, i.e., it holds that $J^{\mathrm{o}}(e(k+1),k+1) \leq \widetilde{J}(e(k+1),k+1)$. From (18), by using (26), one has that

$$\begin{aligned} &\widetilde{J}(e(k+1),k+1) - J^{\mathrm{o}}(e(k),k) \\ &< -\|e(k)\|^2_Q - \|\kappa_{\mathrm{f}}(e(k))\|^2_R - \|v_1(k) + v_2(k) + d(k)\|^2_r < 0 \end{aligned} \tag{30}$$

which implies that J^{o} is a decreasing function. Hence, to conclude, $z = \bar{z}_{\mathrm{ref}}$ is an asymptotically stable equilibrium point of the controlled system. ■

5. SIMULATION RESULTS

In this section the simulation results obtained by applying the proposed hierarchical MPC/SMC scheme to a realistic microgrid scenario are presented, both in GCOM and IOM. The electrical parameters of the simulated system are reported in Table 2. Note that, in IOM the ESu_1 has the most energy capacity C_{ESu_1} and has the role of master unit.

In GCOM, the MPC parameters are chosen such that the matrices are $Q = \mathrm{diag}\,(1, 1, 10^3)$, $R = \mathrm{diag}\,(10^{-2}, 10^{-2}, 10^3)$, $r = 1 \times 10^6$, with $N = 3$ and terminal state weight Π as

$$\Pi = 1 \times 10^5 \begin{bmatrix} 1.9299 & 0.5707 & 0 \\ 0.5707 & 0.1727 & 0 \\ 0 & 0 & 0.01 \end{bmatrix} \tag{31}$$

On the other hand, in IOM, we assume that the DGu and ESus satisfy the microgrid power demand. The MPC is implemented choosing in IOM the matrices $Q = \mathrm{diag}\,(10^8, 10^{-2})$, $R = \mathrm{diag}\,(10^3, 1)$, $r = 1 \times 10^6$ and the terminal state weight Π as

$$\Pi = 1 \times 10^8 \begin{bmatrix} 1 & 0 \\ 0 & 0.0001 \end{bmatrix} \tag{32}$$

For all the simulation tests the sampling time t_{s} has been set equal to 1×10^{-6} s, while the MPC sampling time T is equal to 1 min.

Table 2. Electrical parameters of the microgrid in Figure 1

Quantity	Value	Description
C_{ESu_1}	120 kWh	Energy capacity of ESu_1
C_{ESu_2}	40 kWh	Energy capacity of ESu_2
η_{ESu_1}	0.8	Efficiency of ESu_1
η_{ESu_2}	0.9	Efficiency of ESu_2
$P_{\mathrm{ESu,max}}$	18 kW	Max. power of ESus
$SoC_{\max}$	0.8	Max. SoC of ESus
$SoC_{\min}$	0.2	Min. SoC of ESus
SoC_{ref}	0.7	SoC reference of ESus
$P_{\mathrm{grid,ref}}$	0 kW	Power reference of the grid

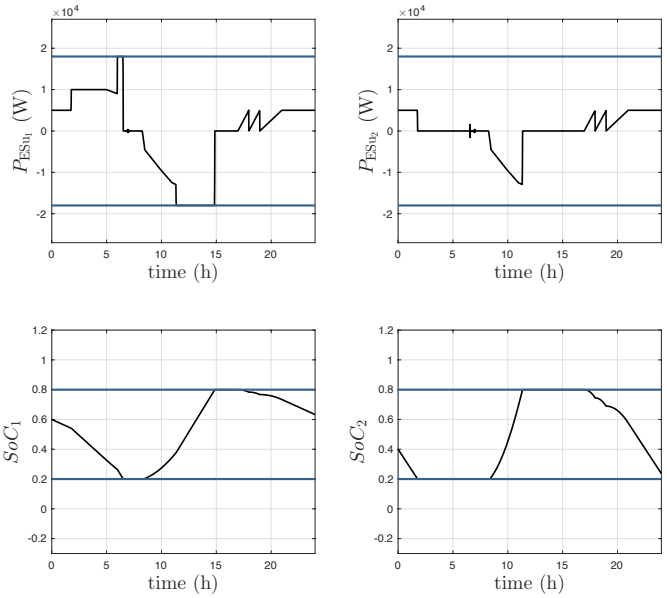

Fig. 4. Power and SoC of ESus in GCOM with constraints visualization.

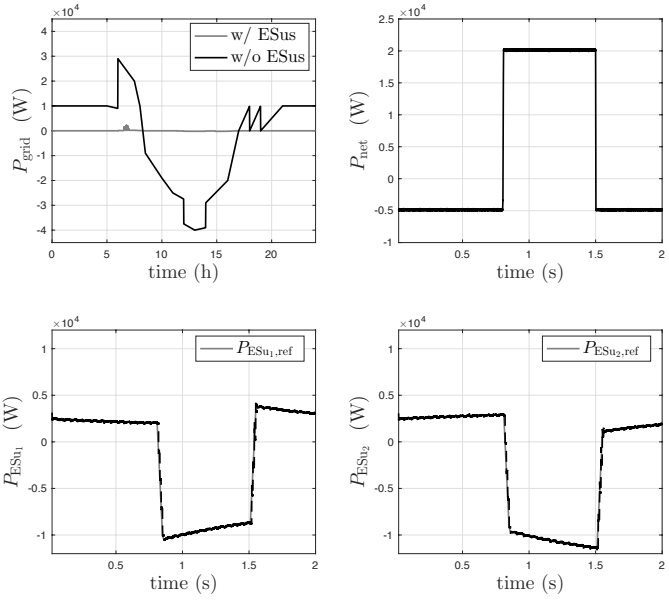

Fig. 5. Power exchanged with the main grid with and without ESus in GCOM, step variation of P_{net}, tracking of $P_{\mathrm{ESu}_1,\mathrm{ref}}$ and of $P_{\mathrm{ESu}_2,\mathrm{ref}}$.

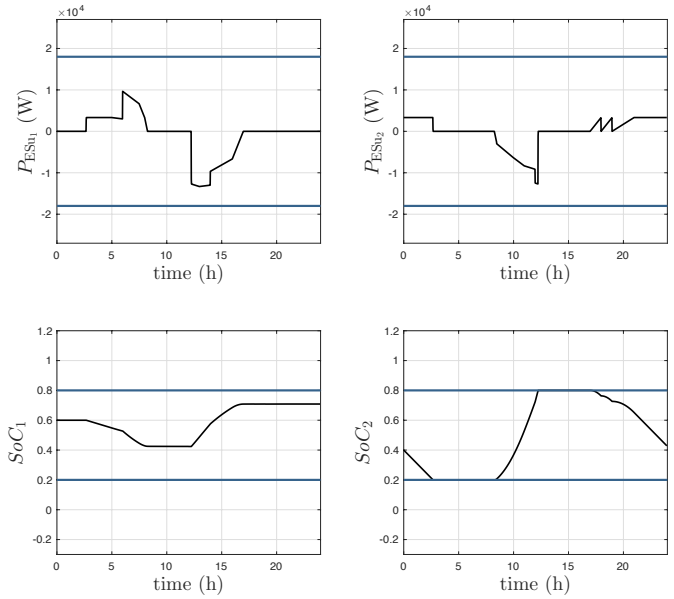

Fig. 6. Power and SoC of ESus in IOM with constraints visualization.

A typical daily behavior has been considered with both load and generation variations. Figure 4 shows the time evolution of the power and of the SoC of the ESus in GCOM. One can observe that the input and state constraints are always satisfied. Moreover, from Figure 5 one can observe that the power exchanged with the main grid P_{grid} is almost zero during all the day when the proposed strategy with ESus is applied. The same figure shows the tracking property of the local SSOSM controllers. In Figure 6, one can observe that the input and state constraints are always fulfilled also in IOM. More specifically, since we have considered the ESu_1 as master unit, as expected, one can observe that the master unit discharges after ESu_2.

6. CONCLUSIONS

In this paper a supervisory control scheme able to optimize the operation of a microgrid, which includes distributed generation units, loads and energy storage units, has been proposed. A high level Model Predictive Control has been designed in order to optimize the operations of the microgrid, taking into account input and states constraints. A Suboptimal Second-Order Sliding Mode controller is used as low level control to track the references generated by the EMS model-based MPC. In this paper the case of a single microgrid associated with the EMS is considered but the proposed strategy can be extended to the more general situations in which several microgrids are managed by a single high level controller. In that case the prediction model has to encompass all the exchanged powers.

REFERENCES

Amin, S. and Wollenberg, B. (2005). Toward a smart grid: power delivery for the 21st century. *IEEE Power Energy Mag.*, 3(5), 34–41. doi:10.1109/MPAE.2005.1507024.

Bartolini, G., Ferrara, A., and Usai, E. (1998). Chattering avoidance by second-order sliding mode control. *IEEE Trans. Automat. Control*, 43(2), 241–246. doi:10.1109/9.661074.

Bouzid, A.M., Guerrero, J.M., Cheriti, A., Bouhamida, M., Sicard, P., and Benghanem, M. (2015). A survey on control of electric power distributed generation systems for microgrid applications. *Renew. Enew. Sust. Energ. Rev.*, 44, 751 – 766. doi:http://dx.doi.org/10.1016/j.rser.2015.01.016.

Cucuzzella, M., Incremona, G.P., and Ferrara, A. (2015a). Design of robust higher order sliding mode control for microgrids. *IEEE J. Emerg. Sel. Topics Circuits Syst.*, 5(3), 393–401. doi:10.1109/JETCAS.2015.2450411.

Cucuzzella, M., Incremona, G.P., and Ferrara, A. (2015b). Master-slave second order sliding mode control for microgrids. In *Proc. IEEE American Control Conf.* Chicago, IL, USA.

Cucuzzella, M., Incremona, G.P., and Ferrara, A. (2015c). Third order sliding mode voltage control in microgrids. In *Proc. IEEE European Control Conf.* Linz, Austria.

Cucuzzella, M., Incremona, G.P., Guastalli, M., and Ferrara, A. (2016). Sliding mode control for maximum power point tracking of photovoltaic inverters in microgrids. In *Proc. IEEE 55th Conf. Decision Control*, 7294–7299. doi: 10.1109/CDC.2016.7799395.

Cucuzzella, M., Trip, S., De Persis, C., and Ferrara, A. (2017). Distributed second order sliding modes for optimal load frequency control. In *Proc. American Control Conf.* Seattle, WA, USA.

Incremona, G.P., Ferrara, A., and Magni, L. (2017a). Asynchronous networked MPC with ISM for uncertain nonlinear systems. *IEEE Trans. Automat. Control*, PP(99), –. doi: 10.1109/TAC.2017.2653760.

Incremona, G.P., Ferrara, A., and Magni, L. (2017b). MPC for robot manipulators with integral sliding modes generation. *IEEE/ASME Trans. Mechatronics*, PP(99), –. doi: 10.1109/TMECH.2017.2674701.

Incremona, G.P., Cucuzzella, M., and Ferrara, A. (2016). Adaptive suboptimal second-order sliding mode control for microgrids. *International Journal of Control*, 1–19. doi: 10.1080/00207179.2016.1138241.

Lasseter, R. (2002). Microgrids. In *IEEE Power Engineering Society Winter Meeting*, volume 1, 305–308. doi: 10.1109/PESW.2002.985003.

Mayne, D.Q. (2014). Model predictive control: Recent developments and future promise. *Automatica*, 50(12), 2967–2986. doi:http://dx.doi.org/10.1016/j.automatica.2014.10.128.

Palma-Behnke, R., Benavides, C., Lanas, F., Severino, B., Reyes, L., Llanos, J., and Saez, D. (2013). A microgrid energy management system based on the rolling horizon strategy. *IEEE Trans. Smart Grid*, 4(2), 996–1006. doi: 10.1109/TSG.2012.2231440.

Rahimi-Eichi, H., Ojha, U., Baronti, F., and Chow, M.Y. (2013). Battery management system: An overview of its application in the smart grid and electric vehicles. *Industrial Electronics Magazine, IEEE*, 7(2), 4–16. doi: 10.1109/MIE.2013.2250351.

Rawlings, J. and Mayne, D. (2009). *Model Predictive Control: Theory and Design*. Nob Hill Pub, Llc.

Tan, K., So, P., Chu, Y., and Chen, M.Z. (2013). Coordinated control and energy management of distributed generation inverters in a microgrid. *IEEE Trans. Power Delivery*, 28(2), 704–713. doi:10.1109/TPWRD.2013.2242495.

Trip, S., Cucuzzella, M., Ferrara, A., and De Persis, C. (2017). An energy function based design of second order sliding modes for automatic generation control. In *Proc. 20th IFAC World Congr.* Toulouse, France.

Utkin, V.I. (1992). *Sliding Modes in Optimization and Control Problems*. Springer Verlag, New York.